iScience

CellPress
OPEN ACCESS

Article

Machine learning models based on fluid immunoproteins that predict non-AIDS adverse events in people with HIV

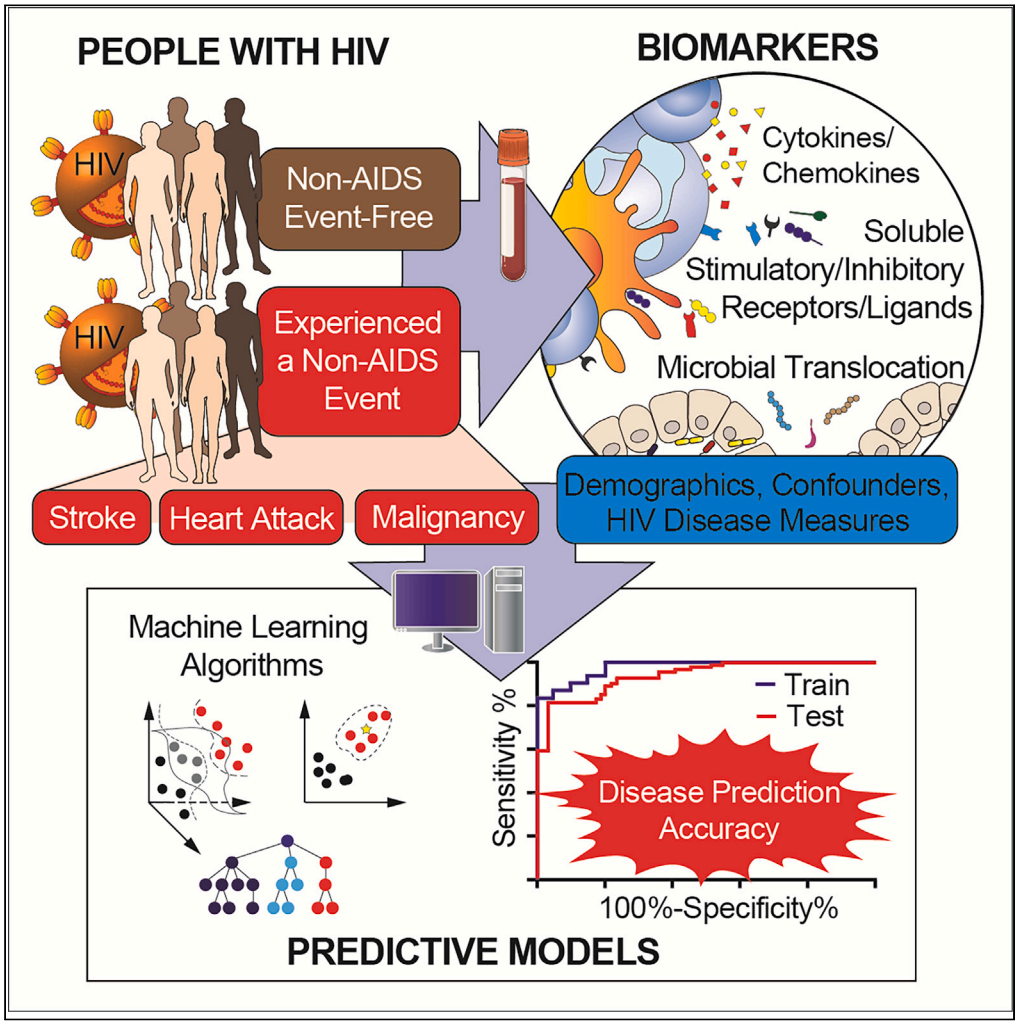

Thomas A. Premeaux, Scott Bowler, Courtney M. Friday, ..., Sara Gianella, Lishomwa C. Ndhlovu, AIDS Clinical Trials Group NWCS 411 study team

tap4002@med.cornell.edu

Highlights

Individual biomarkers are limited in discriminating non-AIDS event risk

Age is a confounder for biomarker trajectories and non-AIDS event classification

Support vector classification models predict non-AIDS events with high accuracy

Premeaux et al., iScience 27, 109945
June 21, 2024
https://doi.org/10.1016/j.isci.2024.109945

iScience

CellPress
OPEN ACCESS

Article

Machine learning models based on fluid immunoproteins that predict non-AIDS adverse events in people with HIV

Thomas A. Premeaux,[1,7,*] Scott Bowler,[1] Courtney M. Friday,[1] Carlee B. Moser,[2] Martin Hoenigl,[3,4] Michael M. Lederman,[5] Alan L. Landay,[6] Sara Gianella,[3] Lishomwa C. Ndhlovu,[1] and for the AIDS Clinical Trials Group NWCS 411 study team

SUMMARY

Despite the success of antiretroviral therapy (ART), individuals with HIV remain at risk for experiencing non-AIDS adverse events (NAEs), including cardiovascular complications and malignancy. Several surrogate immune biomarkers in blood have shown predictive value in predicting NAEs; however, composite panels generated using machine learning may provide a more accurate advancement for monitoring and discriminating NAEs. In a nested case-control study, we aimed to develop machine learning models to discriminate cases (experienced an event) and matched controls using demographic and clinical characteristics alongside 49 plasma immunoproteins measured prior to and post-ART initiation. We generated support vector machine (SVM) classifier models for high-accuracy discrimination of individuals aged 30–50 years who experienced non-fatal NAEs at pre-ART and one-year post-ART. Extreme gradient boosting generated a high-accuracy model at pre-ART, while K-nearest neighbors performed poorly all around. SVM modeling may offer guidance to improve disease monitoring and elucidate potential therapeutic interventions.

INTRODUCTION

The age of people living with HIV (PWH) is steadily rising,[1] and these dynamic changes are projected to continue.[2] Importantly, age-related comorbidities, such as hypertension, diabetes, cardiovascular disease (CVD), and non-AIDS-defining cancers, are occurring more frequently and at an earlier age in PWH despite antiretroviral drug therapy (ART).[3–5] Underlying mechanisms leading to non-AIDS adverse events (NAEs) are multifactorial and may be cumulative, including those due to residual HIV persistence, immune dysregulation, and co-infections.[6,7] While persistent inflammation and immune activation are hallmarks of chronic HIV infection that often remain during ART-mediated viral suppression, these processes can further be compounded by age progression.[8,9] Currently, a lack of additional interventions to ameliorate immune activation and immune dysregulation in PWH on ART warrants further understanding of the underlying processes that may drive NAEs and development of modalities to predict and monitor their occurrence.

The evolution of improved disease models in evaluating mortality and morbidity risk has been invaluable as potential indices for improving the clinical management of PWH.[10,11] Circulating immunoregulatory proteins have emerged as important indicators of HIV immunopathogenesis that may serve as ideal predictive biomarkers for NAEs as they are easily accessible, can capture the overall immune landscape in blood and tissues, and are direct biological effectors. Indeed, many individual biomarkers of inflammation and immune dysfunction have been identified to be independently associated with early mortality and age-related comorbidities[12–15] and as potential predictors for NAEs in PWH.[16–18] Though the network of biological pathways these biomarkers represent does not occur independently, in combination, their effectiveness as monitoring tools in a clinical setting has not been assessed. A machine learning (ML) approach can address this gap as algorithms can assess patterns in data to make predictions. Various ML-based algorithms have been used to reveal biological features in the classification of complex diseases, such as CVD and cancer,[19,20] and predict changes in immune function, disease severity, and mortality risk in infectious diseases.[21–23] Previous studies have used ML to predict comorbid and virological failure outcomes in PWH based strictly with social-demographic and clinical-related variables[24,25]; however, applying an ML approach may be an effective tool to uncover composite

[1]Division of Infectious Diseases, Department of Medicine, Weill Cornell Medicine, New York, NY, USA
[2]Center for Biostatistics in AIDS Research in the Department of Biostatistics, Harvard T.H. Chan School of Public Health, Boston, MA, USA
[3]Division of Infectious Diseases, Department of Medicine, University of California San Diego, San Diego, CA, USA
[4]Division of Infectious Diseases, Department of Internal Medicine, Medical University of Graz, Graz, Austria
[5]Department of Medicine, Division of Infectious Diseases and HIV Medicine, Case Western Reserve University, Cleveland, OH, USA
[6]Department of Internal Medicine, Rush University Medical Center, Chicago, IL, USA
[7]Lead contact
*Correspondence: tap4002@med.cornell.edu
https://doi.org/10.1016/j.isci.2024.109945

immune features that can accurately identify individuals at the highest risk of NAEs and those who could benefit from recurrent clinical monitoring.

Given the increased incidence of age-related comorbidities among PWH even despite effective viral suppression by ART and the limited application of previously identified biomarkers into clinical practice, we aimed to develop ML-driven predictive models for the onset of NAEs. Here, we leveraged the AIDS Clinical Trials Group Longitudinal Linked Randomized Trials (ALLRT) study of PWH prior and post-ART initiation who did or did not experience an NAE. We evaluated circulating proteins associated with inflammation, CVD, myeloid/lymphocyte activation, microbial translocation, or coagulopathy. To infer relationships with disease that are not apparent through traditional statistical approaches, we employed multiple ML algorithms in efforts to generate immunoprotein models, paired with demographic and clinical variables, which are highly accurate in the classification of PWH who experience an NAE.

RESULTS

Study design and participant demographics

Cryopreserved plasma from participants living with HIV from three time points (baseline [pre-ART]: 64 cases, 92 controls; one-year post-ART: 96 cases, 167 controls; and immediately preceding an event: 58 cases, 101 controls) was available. Case and control groups were comparable in age, sex, and $CD4^+$ T cell counts at baseline (pre-ART) and ART regimen at week 48 (protease inhibitor- or abacavir-containing regimens) (Table 1). At study entry, participants were predominately male (83.5%), with a median age of 39 (range 23–69) years, 213 (Q1-Q3: 87–334) $CD4^+$ T cells/μL, and 4.77 (Q1-Q3: 4.38–5.40) $\log_{10}$ copies/mL plasma HIV RNA. Participants had a median $CD4^+$ T cell count at year 1 of 404 (Q1-Q3: 269–561) cells/μL for controls and 213 (Q1-Q3: 87–334) cells/μL for cases. Frequency of specific NAEs among cases includes 13.4% mortality, 26.1% non-fatal myocardial infarction (MI)/stroke, 35.8% non-fatal malignancy, and 24.6% non-fatal serious bacterial infection (Figure S1). NAEs occurred at a median of 2.8 years (Q1-Q3: 1.7–4.6) after ART initiation and 10.5 (Q1-Q3: 6–19) weeks from the pre-event time point.

Exploratory immunoregulatory protein distributions and correlates

Co-activation and dysfunction of T cells, B cells, and natural killer (NK) cell lymphocyte populations can be driven by diverse immunoregulatory receptor and cognate ligand interactions. Soluble forms of these immunoregulatory proteins offering a representation of lymphocyte activation and exhaustion status not limited to the periphery have been shown to play a key role in maintaining immune homeostasis and are suggested as putative markers in pathology in multiple disease states.[26–28] Furthermore, levels of several immunoregulatory proteins associate with viral persistence and T cell function among PWH on ART.[18,29] While we previously identified immunoregulatory proteins that individually predict NAEs, we expand on our findings by employing a 20-plex panel that encompasses shared and unique pathways of innate and adaptive responses, including T cell activation (OX40, 4-1BB)[30,31] and inhibition (V-type immunoglobulin domain-containing suppressor of T cell activation [VISTA], V-set domain containing T cell activation inhibitor 1 [VTCN1]),[32,33] NK cell cytotoxicity (DNAX accessory molecule [DNAM]-1),[34] lectin-mediated inflammation and lymphocyte regulation (Galectins, sialic acid binding Ig-like lectins [Siglecs]),[35,36] and B cell differentiation and proliferation (B cell activating factor [BAFF], a proliferation-inducing ligand [APRIL]).[37] Distributions of these soluble immunoregulatory protein levels for cases and controls at pre-ART, one year post-ART, and pre-event time points are illustrated in Figure 1. Hodges-Lehmann estimates demonstrate many biomarkers are significantly lower at the one year post-ART time point compared to pre-ART measures (Table S1), including noteworthy median differences in both controls and cases for 4-1BB, indoleamine-2,3-deoxygenase 1 [IDO1], and OX40 (all $p < 0.0001$), indicating ART use may impact associated mechanisms. However, the median levels of other immunoregulatory proteins, such as 4-1BBL, remain consistent with ART.

Paucity of individual biomarker differences overall among cases and control

To demonstrate the lack of stringency of a single biomarker in discriminating cases and controls, we evaluated significant differences and the magnitude of change between cases and controls for all individual biomarkers, including newly measured immunoregulatory proteins and biomarkers previously evaluated in this cohort,[16–18] that were available at pre-ART, one year post-ART, and pre-event time points for total and specific non-AIDS events. Together, these 49 plasma biomarkers known to be associated with inflammation, myeloid cell activation, lymphocyte activation, microbial translocation, CVD, or coagulopathy were evaluated (Table S2), many of which were previously identified as potential predictors of NAEs in previous exploratory conditional logistic regression analysis.[16–18] On an independent basis, significant differences in biomarkers including soluble urokinase plasminogen activator receptor (suPAR) and inducible T cell co-stimulator ligand (ICOSL) at baseline; interleukin (IL)-6, CD27, CD14, suPAR, and β-D-glucan (BDG) at year 1; and D-dimer, IL-6, suPAR, BDG, interferon gamma inducible protein 10 (IP-10), lipopolysaccharide-binding protein (LBP), CD27, Siglec-9, tumor necrosis factor receptor 1 (TNFR-1), and VISTA at pre-event (Figure 2; all $p < 0.05$) were observed. However, only pre-event D-dimer and IL-6 p values remained significant when adjusting for multiple testing (false discovery rate [FDR]). Of note, non-significant fold difference decreases in proteins when cases compared to controls were observed, including decreases in 4-1BBL at baseline and pre-event and CD30 at year 1 and pre-event.

ML-driven composite immune biomarker models for total and non-fatal NAEs

To construct predictive ML classification models, we employed commonly used algorithms that implement varying approaches to modeling data that limit computational burden while minimizing redundant analyses. ML algorithms utilized included K-nearest neighbors (KNN),

Table 1. Demographic and clinical characteristics of participants at parent study entry

	Case	Control	Total
Characteristic	(*N* = 134)	(*N* = 267)	(*N* = 401)
Age at parent study entry (years)	46.5 [23–69]	44.0 [23–67]	45.0 [23–69]
Regimens evaluated by parent study			
ACTG 384:(AZT + 3TC vs. d4T + ddI) + (EFV vs. NFV vs. NFV + EFV)/	24 (17.9%)	67 (25.1%)	91 (22.7%)
ACTG 388: (AZT + 3TC vs. d4T + 3TC) + (IDV vs. NFV vs. IDV + NFV)	16 (11.9%)	10 (3.7%)	26 (6.5%)
A5014: NVP + [LPV/r vs. (ABC + 3TC + d4T)]/	2 (1.5%)	5 (1.9%)	7 (1.7%)
A5095: AZT/3TC + (ABC vs. EFV vs. ABC + EFV)/	41 (30.6%)	64 (24.0%)	105 (26.2%)
A5142: (EFV + AZT/d4T + 3TC) vs. (LPV/r + AZT/d4T + 3TC) vs. (EFV + LPV/r)	19 (14.2%)	58 (21.7%)	77 (19.2%)
A5202: (ABC/3TC vs. TFV/FTC) + (ATV/r vs. EFV)	32 (23.9%)	63 (23.6%)	95 (23.7%)
Natal sex			
Male	112 (83.6%)	223 (83.5%)	335 (83.5%)
Female	22 (16.4%)	44 (16.5%)	66 (16.5%)
Race/ethnicity			
White non-Hispanic	70 (52.2%)	126 (47.2%)	196 (48.9%)
Black non-Hispanic	48 (35.8%)	73 (27.3%)	121 (30.2%)
Hispanic (regardless of race)	15 (11.2%)	58 (21.7%)	73 (18.2%)
Other	1 (0.7%)	10 (3.7%)	11 (2.7%)
Baseline $CD4^+$ T cell count (cells/μL)	207 [88, 333]	221 [87, 334]	213 [87, 334]
Baseline $\log_{10}$ HIV-1 RNA (copies/mL)	4.76 [4.39, 5.41]	4.79 [4.37, 5.39]	4.77 [4.38, 5.40]
Chronic hepatitis B/C status	33 (24.6%)	25 (9.4%)	58 (14.5%)
Current or previous injection drug use	17 (12.7%)	22 (8.2%)	39 (9.7%)
Waist-to-hip ratio	0.924 [0.897, 0.972]	0.931 [0.887, 0.973]	0.928 [0.893, 0.973]
History of clinician-diagnosed diabetes	11 (8.2%)	15 (5.6%)	26 (6.5%)
History of hypertension	43 (32.1%)	63 (23.6%)	106 (26.4%)
Use of antihypertensive or lipid lowering agents	30 (22.4%)	44 (16.5%)	74 (18.5%)
Current or past smoker	100 (74.6%)	144 (53.9%)	244 (60.8%)
Family history of myocardial infarction	28 (20.9%)	42 (15.7%)	70 (17.5%)

Categorical variables are represented as frequency (%) and continuous variables as median [Q1, Q3] or median (range). Abbreviations: 3TC, lamivudine; ABC, abacavir; ATZ/r, ritonavir-boosted atazanavir; AZT, zidovudine; d4T, stavudine; ddI, didanosine; EFV, efavirenz; FTC, emtricitabine; IDV, indinavir; LPV/r, ritonavir-boosted lopinavir; NFV, nelfinavir; NVP, nevirapine; TFV, tenofovir.

extreme gradient boosting (XGBoost), and support vector machine classifier (SVM) paired with the following parameters for feature selection: demographics (age and sex), HIV disease measures (pre-ART CD4 count, pre-ART HIV-1 RNA levels), and the 49 plasma biomarkers previously evaluated (Table S2). To preserve the case-control nature of the study, we applied conditional transformation to the dataset.[38] From baseline measures, a KNN model resulted in poor prediction of participant case-control status (receiver operating characteristic area under the curve [AUC-ROC] = 0.633 [0.502, 0.764], Figures 3 and S2). These results were echoed in the XGBoost (AUC-ROC = 0.622 [0.534, 0.791]) and SVM (AUC-ROC = 0.673 [0.545, 0.800]) models. Accuracy increased when evaluating year 1 measures for all models: KNN AUC-ROC = 0.736 [0.643, 0.829], XGBoost AUC-ROC = 0.759 [0.669, 0.849], and SVM AUC-ROC = 0.735 [0.642, 0.828]. However, all models remained poor using pre-event measures: KNN AUC-ROC = 0.679 [0.553, 0.804]), XGBoost AUC-ROC = 0.691 [0.566, 0.815], and SVM AUC-ROC = 0.582 [0.449, 0.715].

When cases were limited to non-fatal events, baseline model performances were mixed (Figures 4 and S3): a simplified KNN model comprised ICOSL, CD73, and age (AUC-ROC = 0.635 [0.494, 0.776]); XGBoost (consisting of lymphocyte-activation gene 3 [LAG3], cytotoxic T-lymphocyte associated protein 4 [CTLA-4], suPAR, and age) produced an AUC-ROC = 0.815 [0.702, 0.929]; and a 31-feature SVM model resulted in AUC-ROC = 0.708 [0.576, 0.841]. To determine if viremic control would improve prediction, models were retrained on non-morbid

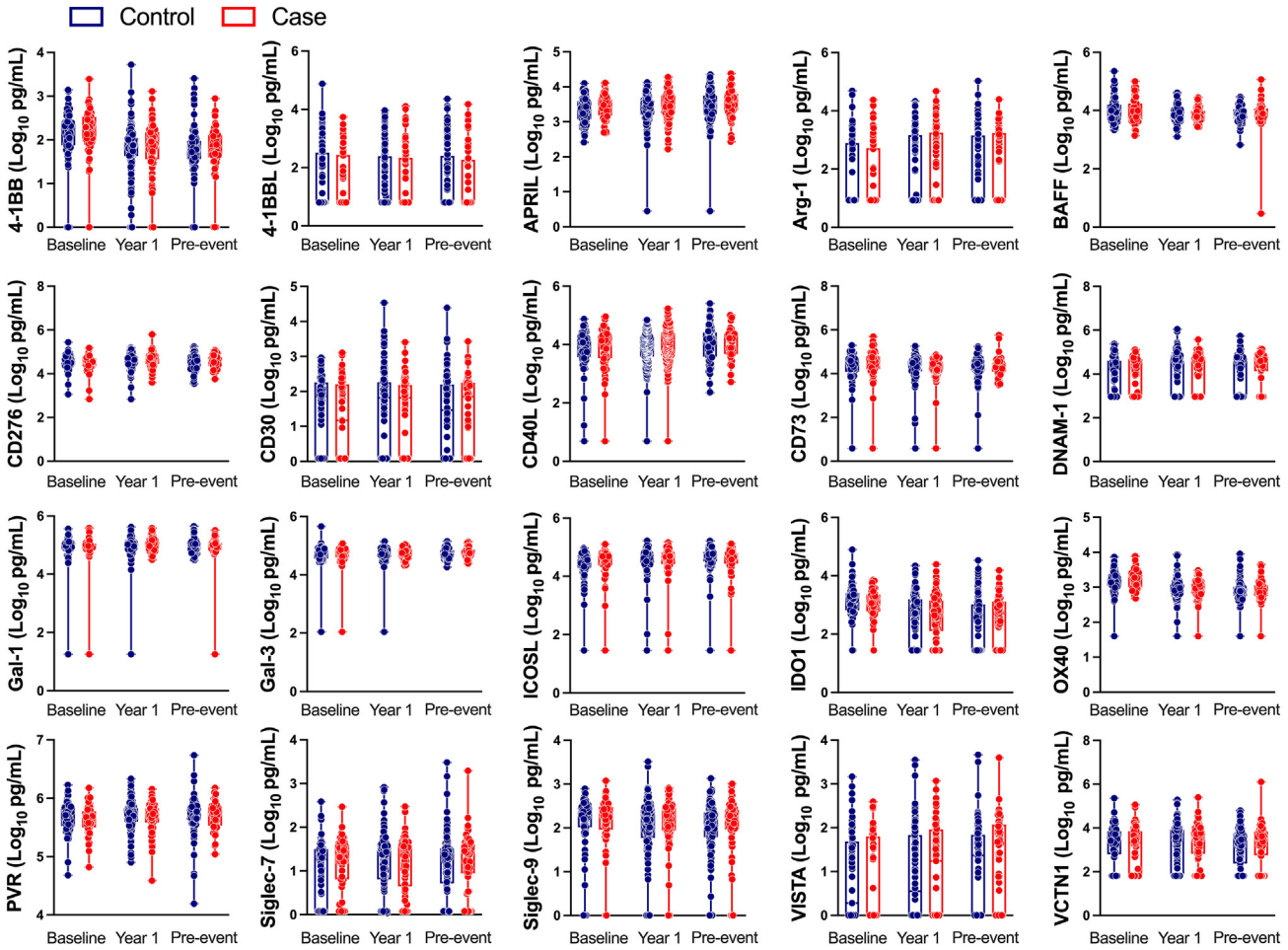

Figure 1. Distributions of evaluated immunoregulatory proteins

Levels among cases (blue) and controls (black) at pre-ART initiation (baseline), a year after ART initiation (year 1), and visit immediately preceding a non-AIDS event (pre-event). Jitter plots including median and interquartile range are displayed. BAFF, B cell activating factor; DNAM-1 DNAX accessory molecule; ICOSL, inducible T cell co-stimulator ligand; IDO1, Indoleamine-2,3-deoxygenase 1; PVR, poliovirus receptor; Siglec, sialic acid binding Ig-like lectin; VISTA, V-type immunoglobulin domain-containing suppressor of T cell activation; VTCN1, V-set domain containing T cell activation inhibitor 1.

datasets generated from the 1 year-post-ART time points. A KNN model consisting of age, sCD14, sTNFR-I, BDG, and CD27 resulted in comparable performance to baseline (AUC-ROC = 0.715 [0.615, 0.815]), and an SVM model (consisting of BDG, CD27, sTNFR-I, and age) resulted in a slightly reduced performance compared to baseline (AUC-ROC = 0.657 [0.551, 0.762]), while the SVM model (CD27, BDG, CD40L, IL-6, sCD14, Arginase-1, CD4 Count, VTCN1, BAFF, sCD40, and CD30) showed improved performance over baseline (AUC-ROC = 0.787 [0.696, 0.878]). At the pre-event time point, all models resulted in reduced performance compared to year 1 (all AUC-ROC $\leq$ 0.624).

Individual biomarker levels demonstrate distinct age trajectories

Immune cell frequency and function as well as circulating immunoprotein profiles are dynamic and vary with age progression.[39–41] Given age-related changes in immunoproteins, the broad age range of the cohort, and age as a common feature included in previous models generated, we next aimed to determine potential age effects on biomarker levels. We evaluated changes in biomarker levels in age differences over 10 years in cases and controls individually to detect changes in the context and absence of non-AIDS events, respectively, at the year 1 visit when all participants were virally suppressed and the slope of decline in immune activation had stabilized.[42] Regression models adjusted for CD4 T cell count between biomarkers and age demonstrated substantial differences in biomarker levels for increasing age among both cases and controls (Figure 5A). However, we also observed a high rate of intragroup variability (i.e., VISTA, cases: mean $\pm$ SD, 5.30 $\pm$ 63.79; IL-6 controls: 2.34 $\pm$ 28.95), demonstrating biomarker level changes with age are not one directional. We next evaluated trends over the 40-year age range spectrum of the cohort. Case/control fold differences in predicted biomarker levels per simulated age values were calculated (Figure 5B), and dramatic fluctuations were observed among many biomarkers over the age spectrum independent of case/control status. The age at which differences in cases and controls inflect or become zero was evaluated

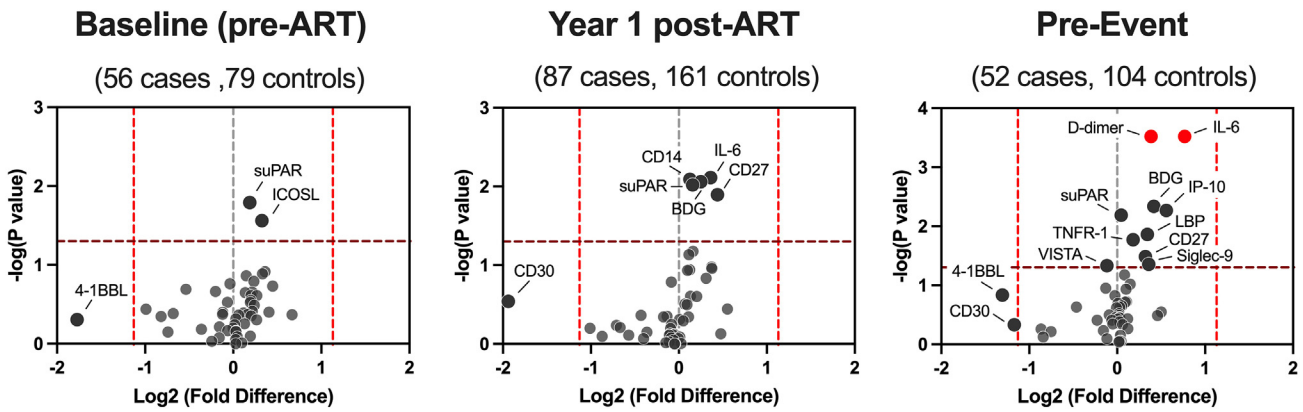

Figure 2. Individual biomarkers and non-AIDS events

Volcano plots showing the estimated fold changes (*x*-axis) versus the -$\log_{10}$ *p* values (*y* axis) for each biomarker among cases and controls at baseline, year 1, and pre-event time points for total non-AIDS events.

(Table S3). These biomarker dynamics with age suggest age restriction criteria may be appropriate when evaluating biomarkers for their predictive efficacy in modeling.

Age-restricted composite immune biomarker ML models predict non-fatal adverse events

Based on the age trajectory analysis, we applied an age restriction criterion of 30–50 years to reduce data noise and re-evaluated all models. At baseline, KNN (featuring D-dimer, IL-6, IP-10, suPAR, CD27, VTCN1, TNFRSF8, Galectin-3, and age) resulted in an AUC-ROC = 0.707 (0.516, 0.897; Figures 6 and S4), comparable to baseline non-age-restricted KNN models, with and without mortal events. XGBoost showed a dramatic increase in performance, featuring Galectin-9, BAFF, and age, resulting in an AUC-ROC = 0.943 (0.861, 1.000), which was less complex but had comparable accuracy to the SVM model (CD40L, CD27, oxidized low-density lipoprotein [oxLDL], CD137, sCD14, intestinal fatty-acid binding protein [I-FABP], suPAR, T cell immunoglobulin mucin 3 [TIM-3], Galectin-3, CD276, CD155, sTNFR-I, Arginase-1, IL-6, and herpesvirus entry mediator [HVEM]; AUC-ROC = 0.952 [0.876, 1.000]). At one year post-ART, KNN (age, CD4 count, D-dimer, sCD14, BDG, CD27, CD276, CD30) produced an AUC-ROC = 0.698 [0.565, 0.830], which was consistent to the XGBoost model (CD4 count, CD276, BDG, suPAR, CD73, CD155, IDO1, APRIL, Galectin-1, TNFSF9, and TNFSRSF8) which resulted in an AUC-ROC = 0.645 (0.507, 0.783). Meanwhile, the SVM model comprising 26 features produced high accuracy classification for cases (AUC-ROC = 0.919 [0.840, 0.998]). At the pre-event time point, a KNN model consisting of age, IP-10, LBP, and CD27 resulted in an AUC-ROC = 0.597 (0.458, 0.736), consistently performing as the weakest of the 3 algorithms tested. XGBoost (featuring BDG, LBP, LAG3, age, VTCN1, and Galectin-1; AUC-ROC = 0.652 [0.479, 0.825]) resulted in performances consistent with KNN except for baseline. SVM, which performed well at baseline and year 1, showed a dramatic decrease in performance at pre-event (AUC-ROC = 0.387 [0.210, 0.565]). Restricting the highest performing model, SVM, to include males only demonstrated reduced accuracy for all three time points (Figure S5).

DISCUSSION

Biomarker feedback was a concept previously discussed to guide approaches to halt HIV disease progression.[43] In this era of ART, elucidating the impact of HIV on a range of NAEs, such as CVD and cancer, can contribute to a more comprehensive and clear characterization for risk. HIV and aging are associated with excess comorbidity, and select immune biomarkers may partially explain these discrepancies. Identifying factors that discriminate PWH at risk of non-communicable disease is an important ongoing area of investigation. In this study, we demonstrate that an ML approach can predict non-fatal NAEs among PWH with high accuracy pre-ART initiation and one-year post-ART at viral suppression. We have presented an integrated computational approach that combines SVM and cross-validation to generate optimal predictive models for non-fatal NAEs among PWH 30–50 years of age. Importantly, immunoproteins were the strongest features, selected over traditional demographic, comorbid, and HIV disease measures, demonstrating the potential importance in the surveillance of these immune parameters.

Given our previous findings on associations between immunoregulatory proteins and morbidity in HIV,[18] we implemented here an expanded panel of biomarkers linked to lymphocyte overactivation and exhaustion. Elevation of soluble immune checkpoints in the plasma not only affects the development, prognosis, and treatment of cancer[26] but is also shown to predict the trajectory of cardiovascular complications.[44,45] However, soluble immune checkpoints have also been shown to be associated with disease outcomes in other viral infections, including human T-lymphotropic virus type 1 (HTLV-1) and severe acute respiratory syndrome coronavirus 2 (SARS-CoV-2).[46–48] While these biomarkers are not restricted to HIV, they could allude to immune perturbations that would lead to morbidity development. Furthermore, it would be optimal to determine whether the panel of biomarkers we evaluated paired with our ML approach can assess morbidity events that occur in other viral infections, or rather our findings are specific to HIV.

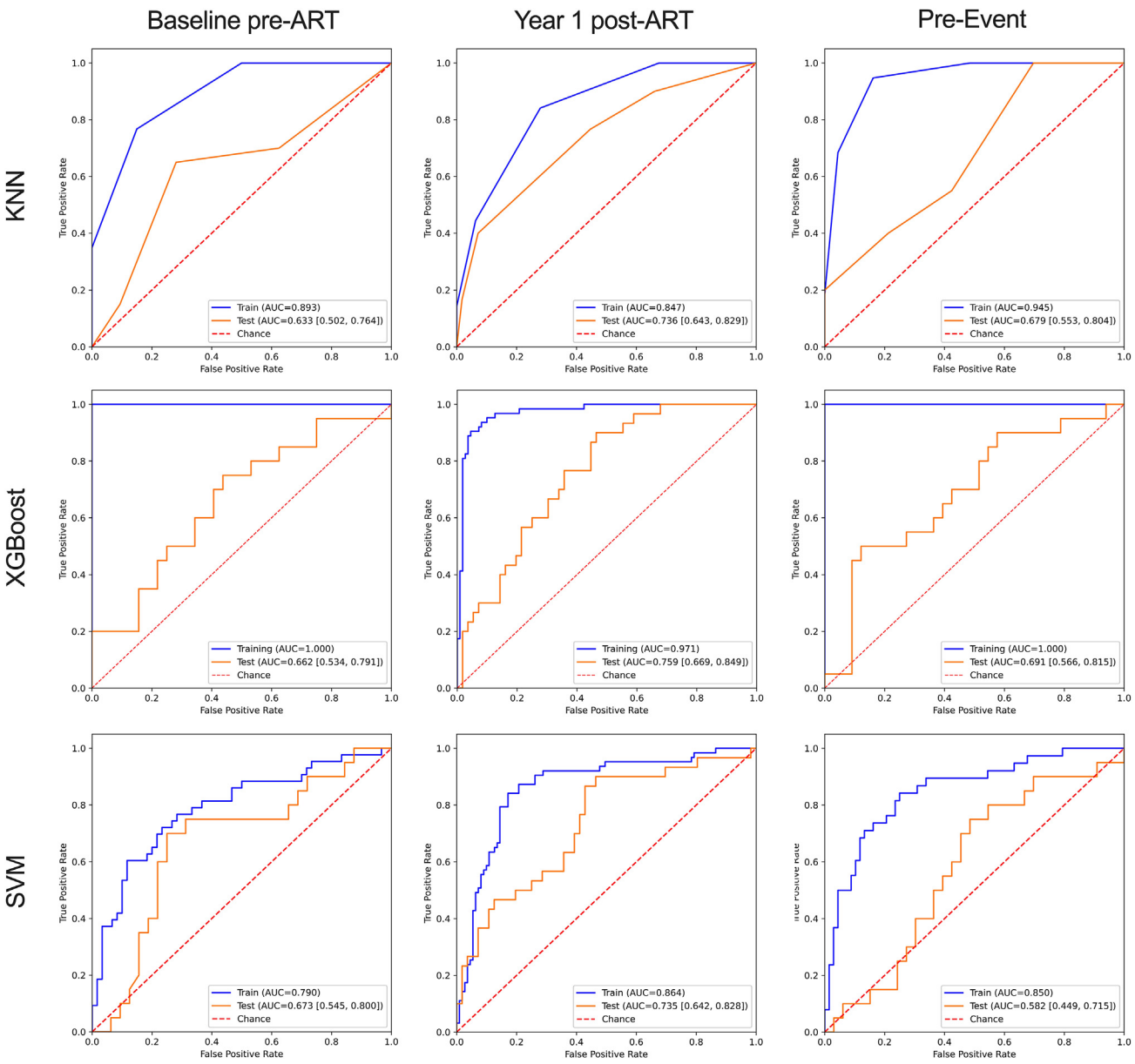

Figure 3. Machine learning classification models of total non-AIDS adverse events

ROC curves illustrating KNN, XGBoost, and support vector machine classification model results in predicting total NAEs (fatal and non-fatal) using biomarkers measures at baseline (pre-ART), year 1 (post-ART), or pre-event. Receiver operating characteristic area under the curve (AUC-ROC) measuring model accuracy for training and test sets is detailed in legend.

ML algorithms have several strengths which make them suitable for complex applications and identifying individuals at risk for disease.[49,50] ML provides increased flexibility and a higher level of interpretability and is free from standard assumptions typical with traditional statistics.[51] Previous studies have generated ML models using a variety of features, including patient demographics, clinical tests, and genetic data, for disease classification, risk, and therapeutic response for several infectious and age-related diseases.[21,52–56] However, determining the most appropriate ML algorithm is integral and ideally based upon the consideration of data features and project requirements. We assessed multiple ML classification methods, including KNN, XGBoost, and SVM, which each represents a variety of linear and non-linear approaches. KNN represents a simple, yet versatile, approach to non-linear classification at the expense of computational cost, memory, sensitivity to *k* choice, and susceptibility to dimensionality, whereas SVM's linear approach excels on data with clear separation between classes and is more effective in high-dimensional space where dimensions exceed sample observations but suffers with large datasets and lacks a probabilistic interpretation. Finally, XGBoost decision trees perform well on non-linear, non-monotonic data or data with segregated clusters and do not

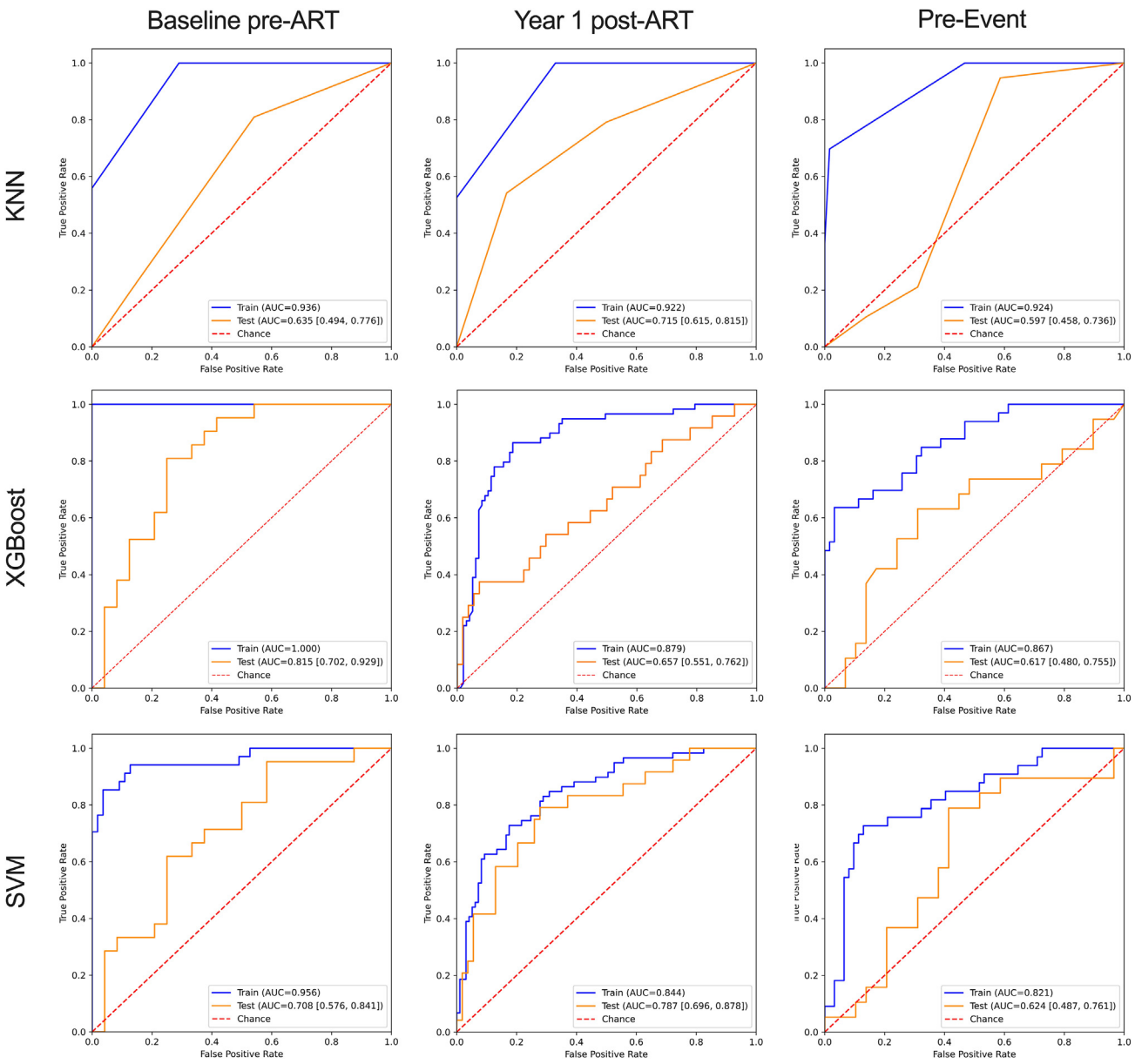

Figure 4. Machine learning classification models of non-fatal adverse events

ROC curves illustrating k-nearest neighbors (KNN), extreme gradient boosting (XGBoost), or support vector machine (SVM) classification model results in predicting non-fatal NAEs using biomarkers measures at baseline (pre-ART), year 1 (post-ART), and pre-event. Receiver operating characteristic area under the curve (AUC-ROC) measuring model accuracy for training and test sets is detailed in legend.

require normalized features. These characteristics help XGBoost boast high accuracy, quickness, and efficiency, while maintaining flexibility, but come at the increased cost of complexity of implementation, memory demands, and interpretability. In this study, KNN consistently underperformed suggesting our dataset did not conform well to non-linear space resulting in the low AUC-ROC observed. This observation is further supported by the exceptional performance we observed of SVM, which does not utilize non-linear space. While there are several approaches in modeling high-dimensional data in linear and non-linear spaces, the potential increase in accuracy would be minimal compared to the additional investment of time and computational resources. Our results overall indicate, among models tested, SVM is the ideal approach for a linear case/control analysis for high prediction accuracy for NAEs and evaluating measures early on during viremia or a year post-ART initiation.

Aging alone is a complex process, and effects on the immune system can manifest at multiple levels, including reduced production and functional capacity of lymphocytes and chronic low-grade inflammation that heightens with age.[57–59] Circulating immunoproteins in plasma

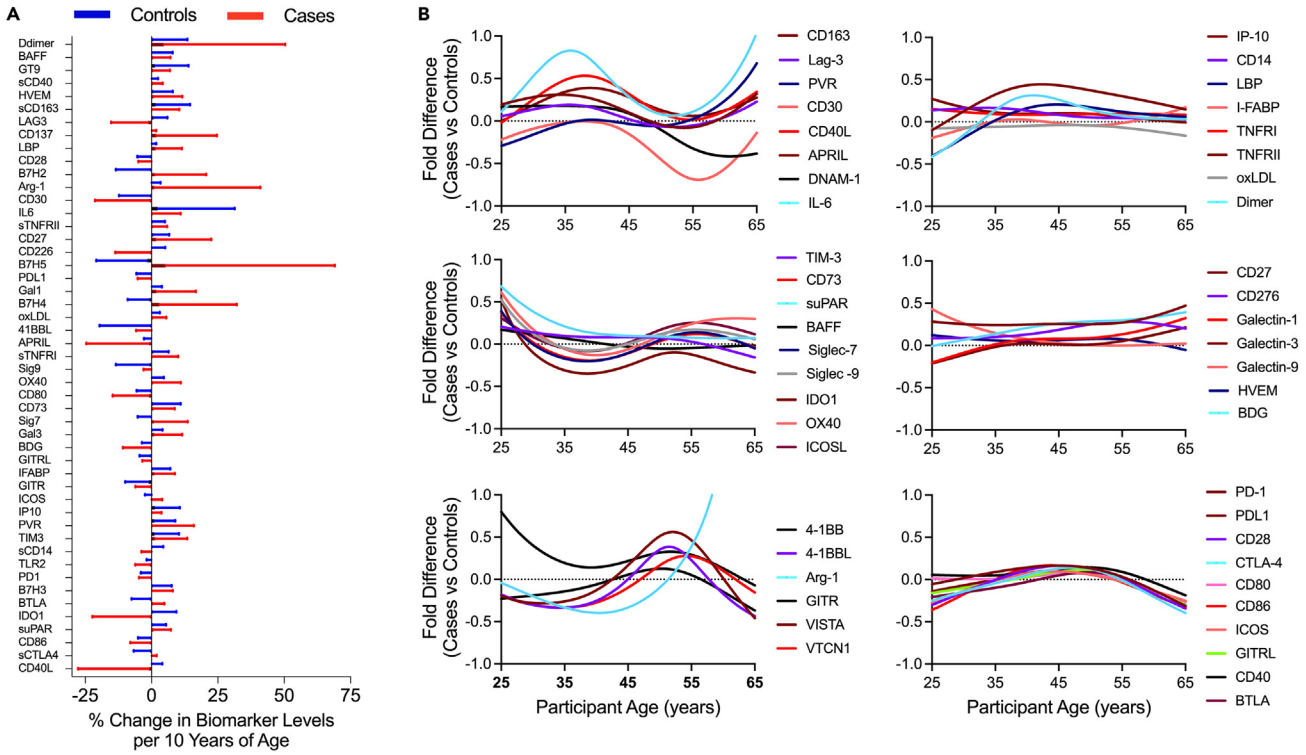

Figure 5. Biomarker changes with age among cases and controls at one-year post-ART initiation

(A) Average biomarker increase for an age difference of 10 years. Relationship between each biomarker and age was assessed via Gaussian linear regression model adjusted for CD4 T cell count.

(B) Predicted biomarker concentrations and simulated age values were used to create scatterplots with 4-knotted splines and calculate fold differences between cases and controls.

can also reflect or influence these age-associated changes of immune function and dramatically change in quantity with age progression. Indeed, our results are consistent with the literature detailing individual biomarker levels are dynamic with age.[40] These changes with age were also demonstrated to differ significantly in individuals that experience NAEs, suggesting the capacity of these markers in disease prediction may be age dependent. Furthermore, unique non-linear patterns in proteins across a 40 years age range with waves of changes depending on the decade of life were observed, similar patterns seen in other studies outside the context of HIV.[60] Finally, the age restriction we implemented for NAE prediction significantly increased model accuracy. As PWH experience the development of age-related comorbidities earlier in life, it is logical to monitor these immune parameters prior to the age of morbidity onset observed in the general population.

In summary, we investigated the potential of applying ML models in predicting NAEs. These strategies may serve as optimal predictors and monitoring tools representative of a real-world scenario once these findings are further validated in larger cohort studies. This will allow the confirmation of these models at various stages of disease progression and ART exposure and their potential as surrogates for clinical trial endpoints. While we limited model generation using primarily immunoprotein data, a multi-omic approach evaluating other parameters, such as cellular senescence, DNA methylation, and glycosylation, and/or the inclusion of traditional measures of morbidity, such as clinical indices of CVD, may delineate higher-accuracy models and reveal additional potential mechanisms at play during disease progression.

Limitations of the study

While the study herein described ML-driven high-accuracy predictive models for NAEs, there are several key limitations, including common caveats of case/control retrospective studies. Case and matched control numbers varied among time points due to specimen availability. ART regimens no longer recommended were in use while current first-line regimens were limited, and many participants demonstrated relatively low $CD4^+$ T cell reconstitution. Our analyses were conducted on a case-control dataset, which does not represent a random sampling of the study population. Secondary cohorts of PWH or people without HIV who experienced similar events were not available for comparison. Conditional transformations were applied to the dataset to preserve these relationships for the ML models; however further evaluation within a cohort study would be beneficial. Classification models were not implemented for biomarker discovery but rather assess potential biomarkers selected by feature selection that are informative in classifying disease from non-disease states. As women were underrepresented, it impacted our ability to adjust for sex, which is significant as sex differences are observed in circulating protein abundance and HIV manifestations.[61–63] Models built to only include males demonstrated lower accuracy, most likely due to further decreasing dataset size. However, sex

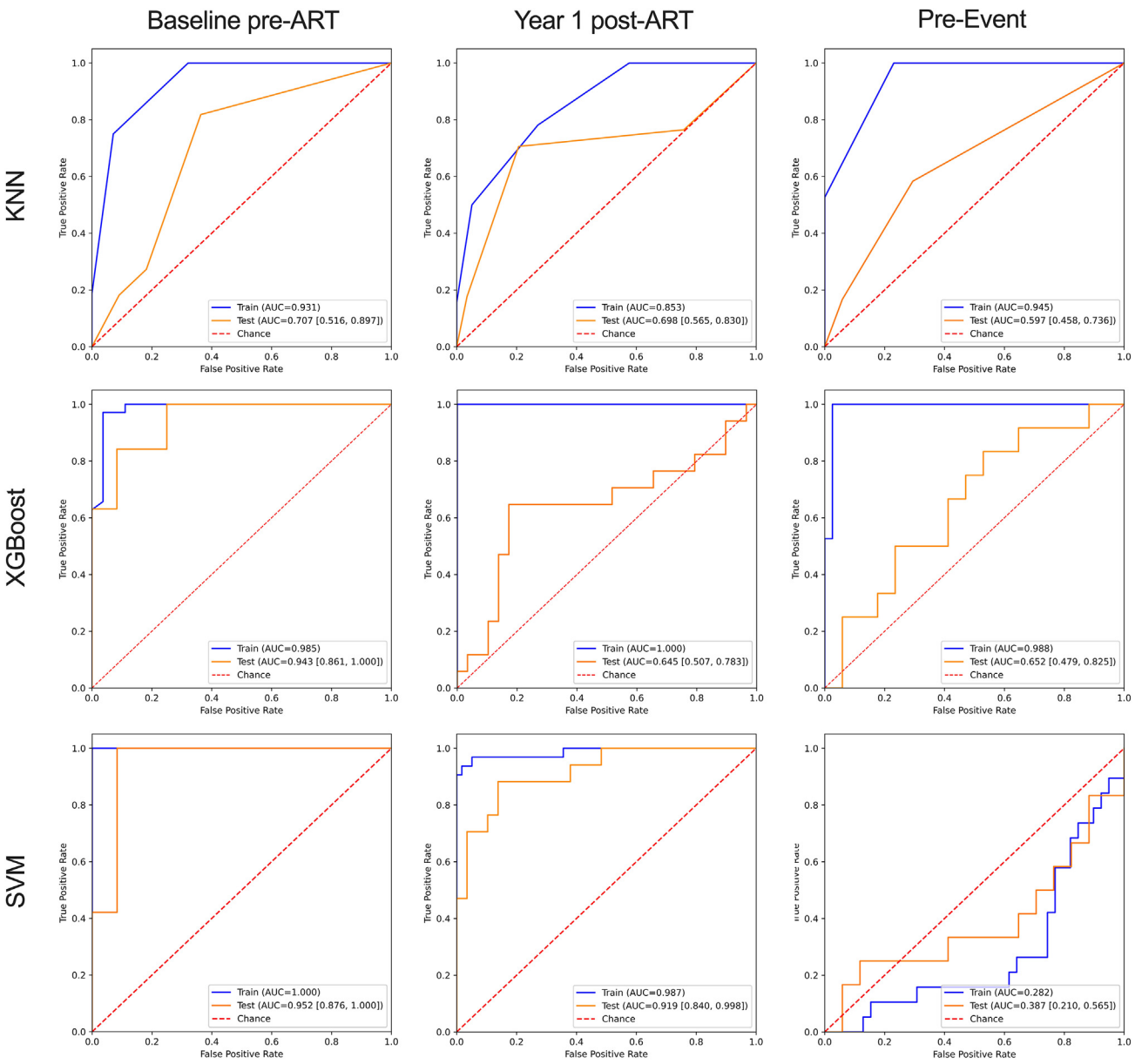

Figure 6. Age-restricted ML classification models of non-fatal adverse events

ROC curves illustrating k-nearest neighbors (KNN), extreme gradient boosting (XGBoost), or support vector machine (SVM) classification model results in predicting total non-AIDS events using biomarkers measures at baseline (pre-ART), year 1 (post-ART), or pre-event. Receiver operating characteristic area under the curve (AUC-ROC) measuring model accuracy for training and test sets is detailed in legend.

was included as a variable in generated models but was not selected as a significant feature, suggesting removing female participants merely reduces power rather than a confounding variable. Additionally, predicting cancer or MI/stroke individually was not feasible due to the limited number of cases and controls for the respective specific event and the risk of model overfitting.

STAR★METHODS

Detailed methods are provided in the online version of this paper and include the following:

- KEY RESOURCES TABLE
- RESOURCE AVAILABILITY
  - Lead contact

SUPPLEMENTAL INFORMATION

Supplemental information can be found online at https://doi.org/10.1016/j.isci.2024.109945.

ACKNOWLEDGMENTS

We would like to thank all study participants and clinical staff involved in the ACTG ALLRT study and the James B. Pendleton Charitable Trust. This research was supported by the National Institutes of Health (NIH) grants R01MH112457 (L.C.N.), R01AI147821 (S.G.), DA051915 (S.G.), UM1AI068634 (C.B.M.), UM1AI068636, and UM1AI106701. The content is solely the responsibility of the authors and does not necessarily represent the official views of the NIH. The funders had no role in the study design, study management, data collection, data analysis, data interpretation, and writing of the manuscript.

AUTHOR CONTRIBUTIONS

T.A.P. and L.C.N. designed the study and concept. T.A.P. and C.M.F. performed the experiments. T.A.P. and S.B. performed the data analysis and interpretation. All authors contributed to the writing and overview of the manuscript.

DECLARATION OF INTERESTS

L.C.N. has served on an advisory board for AbbVie, ViiV, and CytoDyn for work unrelated to this project. M.H. has received project funding from Gilead, Pfizer, and Astellas. M.M.L. has consulted for Lilly and has received competitive grant funding from Gilead for unrelated work.

Received: October 30, 2023
Revised: March 12, 2024
Accepted: May 6, 2024
Published: May 8, 2024

REFERENCES

1. Centers for Disease Control and Prevention (2020). HIV Surveillance Report, *33*. https://www.cdc.gov/hiv/statistics/overview/index.html.
2. Smit, M., Brinkman, K., Geerlings, S., Smit, C., Thyagarajan, K., Sighem, A.v., de Wolf, F., and Hallett, T.B.; ATHENA Observational Cohort (2015). Future challenges for clinical care of an ageing population infected with HIV: a modelling study. Lancet Infect. Dis. *15*, 810–818. https://doi.org/10.1016/S1473-3099(15)00056-0.
3. Shepherd, L., Borges, Á., Ledergerber, B., Domingo, P., Castagna, A., Rockstroh, J., Knysz, B., Tomazic, J., Karpov, I., Kirk, O., et al. (2016). Infection-related and -unrelated malignancies, HIV and the aging population. HIV Med. *17*, 590–600. https://doi.org/10.1111/hiv.12359.
4. Yuan, T., Hu, Y., Zhou, X., Yang, L., Wang, H., Li, L., Wang, J., Qian, H.Z., Clifford, G.M., and Zou, H. (2022). Incidence and mortality of non-AIDS-defining cancers among people living with HIV: A systematic review and meta-analysis. EClinicalMedicine *52*, 101613. https://doi.org/10.1016/j.eclinm.2022.101613.
5. So-Armah, K., Benjamin, L.A., Bloomfield, G.S., Feinstein, M.J., Hsue, P., Njuguna, B., and Freiberg, M.S. (2020). HIV and cardiovascular disease. Lancet. HIV *7*, e279–e293. https://doi.org/10.1016/S2352-3018(20)30036-9.
6. Deeks, S.G., Tracy, R., and Douek, D.C. (2013). Systemic effects of inflammation on health during chronic HIV infection. Immunity *39*, 633–645. https://doi.org/10.1016/j.immuni.2013.10.001.
7. Schouten, J., Wit, F.W., Stolte, I.G., Kootstra, N.A., van der Valk, M., Geerlings, S.E., Prins, M., and Reiss, P.; AGEhIV Cohort Study Group (2014). Cross-sectional comparison of the prevalence of age-associated comorbidities and their risk factors between HIV-infected and uninfected individuals: the AGEhIV cohort study. Clin. Infect. Dis. *59*, 1787–1797. https://doi.org/10.1093/cid/ciu701.
8. Franceschi, C., Bonafè, M., Valensin, S., Olivieri, F., De Luca, M., Ottaviani, E., and De Benedictis, G. (2000). Inflamm-aging. An evolutionary perspective on immunosenescence. Ann. N. Y. Acad. Sci. *908*, 244–254. https://doi.org/10.1111/j.1749-6632.2000.tb06651.x.
9. Deeks, S.G. (2011). HIV infection, inflammation, immunosenescence, and aging. Annu. Rev. Med. *62*, 141–155. https://doi.org/10.1146/annurev-med-042909-093756.
10. Marquine, M.J., Umlauf, A., Rooney, A.S., Fazeli, P.L., Gouaux, B.D., Paul Woods, S., Letendre, S.L., Ellis, R.J., Grant, I., and Moore, D.J.; HIV Neurobehavioral Research Program HNRP Group (2014). The veterans aging cohort study index is associated with concurrent risk for neurocognitive impairment. J. Acquir. Immune Defic. Syndr. *65*, 190–197. https://doi.org/10.1097/QAI.0000000000000008.
11. Soares, C., Kwok, M., Boucher, K.A., Haji, M., Echouffo-Tcheugui, J.B., Longenecker, C.T., Bloomfield, G.S., Ross, D., Jutkowtiz, E., Sullivan, J.L., et al. (2023). Performance of Cardiovascular Risk Prediction Models Among People Living With HIV: A Systematic Review and Meta-analysis. JAMA Cardiol. *8*, 139–149. https://doi.org/10.1001/jamacardio.2022.4873.
12. Boulware, D.R., Hullsiek, K.H., Puronen, C.E., Rupert, A., Baker, J.V., French, M.A., Bohjanen, P.R., Novak, R.M., Neaton, J.D., and Sereti, I.; INSIGHT Study Group (2011). Higher levels of CRP, D-dimer, IL-6, and hyaluronic acid before initiation of antiretroviral therapy (ART) are associated with increased risk of AIDS or death. J. Infect. Dis. *203*, 1637–1646. https://doi.org/10.1093/infdis/jir134.
13. Duprez, D.A., Neuhaus, J., Kuller, L.H., Tracy, R., Belloso, W., De Wit, S., Drummond, F., Lane, H.C., Ledergerber, B., Lundgren, J., et al. (2012). Inflammation, coagulation and cardiovascular disease in HIV-infected individuals. PLoS One *7*, e44454. https://doi.org/10.1371/journal.pone.0044454.
14. Baker, J.V., Sharma, S., Grund, B., Rupert, A., Metcalf, J.A., Schechter, M., Munderi, P., Aho, I., Emery, S., Babiker, A., et al. (2017).

Systemic Inflammation, Coagulation, and Clinical Risk in the START Trial. Open Forum Infect. Dis. *4*, ofx262. https://doi.org/10.1093/ofid/ofx262.

15. Hunt, P.W., Sinclair, E., Rodriguez, B., Shive, C., Clagett, B., Funderburg, N., Robinson, J., Huang, Y., Epling, L., Martin, J.N., et al. (2014). Gut epithelial barrier dysfunction and innate immune activation predict mortality in treated HIV infection. J. Infect. Dis. *210*, 1228–1238. https://doi.org/10.1093/infdis/jiu238.
16. Tenorio, A.R., Zheng, Y., Bosch, R.J., Krishnan, S., Rodriguez, B., Hunt, P.W., Plants, J., Seth, A., Wilson, C.C., Deeks, S.G., et al. (2014). Soluble markers of inflammation and coagulation but not T-cell activation predict non-AIDS-defining morbid events during suppressive antiretroviral treatment. J. Infect. Dis. *210*, 1248–1259. https://doi.org/10.1093/infdis/jiu254.
17. Hoenigl, M., Moser, C.B., Funderburg, N., Bosch, R., Kantor, A., Zhang, Y., Eugen-Olsen, J., Finkelman, M., Reiser, J., Landay, A., et al. (2019). Soluble Urokinase Plasminogen Activator Receptor Is Predictive of Non-AIDS Events During Antiretroviral Therapy-mediated Viral Suppression. Clin. Infect. Dis. *69*, 676–686. https://doi.org/10.1093/cid/ciy966.
18. Premeaux, T.A., Moser, C.B., McKhann, A., Hoenigl, M., Yeung, S.T., Pang, A.P.S., Corley, M.J., Lederman, M.M., Landay, A.L., Gianella, S., and Ndhlovu, L.C. (2022). Monitoring Circulating Immune Checkpoint Proteins as Predictors of Non-AIDS Morbid Events in People With HIV Initiating Antiretroviral Therapy. Open Forum Infect. Dis. *9*, ofab570. https://doi.org/10.1093/ofid/ofab570.
19. Iqbal, M.J., Javed, Z., Sadia, H., Qureshi, I.A., Irshad, A., Ahmed, R., Malik, K., Raza, S., Abbas, A., Pezzani, R., and Sharifi-Rad, J. (2021). Clinical applications of artificial intelligence and machine learning in cancer diagnosis: looking into the future. Cancer Cell Int. *21*, 270. https://doi.org/10.1186/s12935-021-01981-1.
20. Leibovici, L., Paul, M., Nielsen, A.D., Tacconelli, E., and Andreassen, S. (2007). The TREAT project: decision support and prediction using causal probabilistic networks. Int. J. Antimicrob. Agents *30*, S93–S102. https://doi.org/10.1016/j.ijantimicag.2007.06.035.
21. Moulaei, K., Shanbehzadeh, M., Mohammadi-Taghiabad, Z., and Kazemi-Arpanahi, H. (2022). Comparing machine learning algorithms for predicting COVID-19 mortality. BMC Med. Inf. Decis. Making *22*, 2. https://doi.org/10.1186/s12911-021-01742-0.
22. Li, B., Li, M., Song, Y., Lu, X., Liu, D., He, C., Zhang, R., Wan, X., Zhang, R., Sun, M., et al. (2022). Construction of Machine Learning Models to Predict Changes in Immune Function Using Clinical Monitoring Indices in HIV/AIDS Patients After 9.9-Years of Antiretroviral Therapy in Yunnan, China. Front. Cell. Infect. Microbiol. *12*, 867737. https://doi.org/10.3389/fcimb.2022.867737.
23. Bowler, S., Papoutsoglou, G., Karanikas, A., Tsamardinos, I., Corley, M.J., and Ndhlovu, L.C. (2022). A machine learning approach utilizing DNA methylation as an accurate classifier of COVID-19 disease severity. Sci. Rep. *12*, 17480. https://doi.org/10.1038/s41598-022-22201-4.
24. Yang, X., Zhang, J., Chen, S., Weissman, S., Olatosi, B., and Li, X. (2021). Utilizing electronic health record data to understand comorbidity burden among people living with HIV: a machine learning approach. AIDS *35*, S39–S51. https://doi.org/10.1097/QAD.0000000000002736.
25. Mamo, D.N., Yilma, T.M., Fekadie, M., Sebastian, Y., Bizuayehu, T., Melaku, M.S., and Walle, A.D. (2023). Machine learning to predict virological failure among HIV patients on antiretroviral therapy in the University of Gondar Comprehensive and Specialized Hospital, in Amhara Region, Ethiopia, 2022. BMC Med. Inf. Decis. Making *23*, 75. https://doi.org/10.1186/s12911-023-02167-7.
26. Gu, D., Ao, X., Yang, Y., Chen, Z., and Xu, X. (2018). Soluble immune checkpoints in cancer: production, function and biological significance. J. Immunother. Cancer *6*, 132. https://doi.org/10.1186/s40425-018-0449-0.
27. Li, W., Xia, Y., Yang, J., Guo, H., Sun, G., Sanyal, A.J., Shah, V.H., Lou, Y., Zheng, X., Chalasani, N., and Yu, Q. (2020). Immune Checkpoint Axes Are Dysregulated in Patients With Alcoholic Hepatitis. Hepatol. Commun. *4*, 588–605. https://doi.org/10.1002/hep4.1475.
28. Riva, A., and Chokshi, S. (2018). Immune checkpoint receptors: homeostatic regulators of immunity. Hepatol. Int. *12*, 223–236. https://doi.org/10.1007/s12072-018-9867-9.
29. Chiu, C.Y., Schou, M.D., McMahon, J.H., Deeks, S.G., Fromentin, R., Chomont, N., Wykes, M.N., Rasmussen, T.A., and Lewin, S.R. (2023). Soluble immune checkpoints as correlates for HIV persistence and T cell function in people with HIV on antiretroviral therapy. Front. Immunol. *14*, 1123342. https://doi.org/10.3389/fimmu.2023.1123342.
30. Otano, I., Azpilikueta, A., Glez-Vaz, J., Alvarez, M., Medina-Echeverz, J., Cortés-Domínguez, I., Ortiz-de-Solorzano, C., Ellmark, P., Fritzell, S., Hernandez-Hoyos, G., et al. (2021). CD137 (4-1BB) costimulation of CD8(+) T cells is more potent when provided in cis than in trans with respect to CD3-TCR stimulation. Nat. Commun. *12*, 7296. https://doi.org/10.1038/s41467-021-27613-w.
31. Croft, M., So, T., Duan, W., and Soroosh, P. (2009). The significance of OX40 and OX40L to T-cell biology and immune disease. Immunol. Rev. *229*, 173–191. https://doi.org/10.1111/j.1600-065X.2009.00766.x.
32. Lines, J.L., Pantazi, E., Mak, J., Sempere, L.F., Wang, L., O'Connell, S., Ceeraz, S., Suriawinata, A.A., Yan, S., Ernstoff, M.S., and Noelle, R. (2014). VISTA is an immune checkpoint molecule for human T cells. Cancer Res. *74*, 1924–1932. https://doi.org/10.1158/0008-5472.CAN-13-1504.
33. Prasad, D.V.R., Richards, S., Mai, X.M., and Dong, C. (2003). B7S1, a novel B7 family member that negatively regulates T cell activation. Immunity *18*, 863–873. https://doi.org/10.1016/s1074-7613(03)00147-x.
34. Cifaldi, L., Doria, M., Cotugno, N., Zicari, S., Cancrini, C., Palma, P., and Rossi, P. (2019). DNAM-1 Activating Receptor and Its Ligands: How Do Viruses Affect the NK Cell-Mediated Immune Surveillance during the Various Phases of Infection? Int. J. Mol. Sci. *20*, 3715. https://doi.org/10.3390/ijms20153715.
35. Vasta, G.R. (2009). Roles of galectins in infection. Nat. Rev. Microbiol. *7*, 424–438. https://doi.org/10.1038/nrmicro2146.
36. Crocker, P.R., Paulson, J.C., and Varki, A. (2007). Siglecs and their roles in the immune system. Nat. Rev. Immunol. *7*, 255–266. https://doi.org/10.1038/nri2056.
37. Vincent, F.B., Saulep-Easton, D., Figgett, W.A., Fairfax, K.A., and Mackay, F. (2013). The BAFF/APRIL system: emerging functions beyond B cell biology and autoimmunity. Cytokine Growth Factor Rev. *24*, 203–215. https://doi.org/10.1016/j.cytogfr.2013.04.003.
38. Stanfill, B., Reehl, S., Bramer, L., Nakayasu, E.S., Rich, S.S., Metz, T.O., Rewers, M., and Webb-Robertson, B.J.; TEDDY Study Group (2019). Extending Classification Algorithms to Case-Control Studies. Biomed. Eng. Comput. Biol. *10*, 1179597219858954. https://doi.org/10.1177/1179597219858954.
39. Kroll, K.W., Shah, S.V., Lucar, O.A., Premeaux, T.A., Shikuma, C.M., Corley, M.J., Mosher, M., Woolley, G., Bowler, S., Ndhlovu, L.C., and Reeves, R.K. (2022). Mucosal-homing natural killer cells are associated with aging in persons living with HIV. Cell Rep. Med. *3*, 100773. https://doi.org/10.1016/j.xcrm.2022.100773.
40. Glei, D.A., Goldman, N., Lin, Y.H., and Weinstein, M. (2011). Age-Related Changes in Biomarkers: Longitudinal Data from a Population-Based Sample. Res. Aging *33*, 312–326. https://doi.org/10.1177/0164027511399105.
41. Erbe, R., Wang, Z., Wu, S., Xiu, J., Zaidi, N., La, J., Tuck, D., Fillmore, N., Giraldo, N.A., Topper, M., et al. (2021). Evaluating the impact of age on immune checkpoint therapy biomarkers. Cell Rep. *37*, 110033. https://doi.org/10.1016/j.celrep.2021.110033.
42. Gandhi, R.T., Spritzler, J., Chan, E., Asmuth, D.M., Rodriguez, B., Merigan, T.C., Hirsch, M.S., Shafer, R.W., Robbins, G.K., and Pollard, R.B.; ACTG 384 Team (2006). Effect of baseline- and treatment-related factors on immunologic recovery after initiation of antiretroviral therapy in HIV-1-positive subjects: results from ACTG 384. J. Acquir. Immune Defic. Syndr. *42*, 426–434. https://doi.org/10.1097/01.qai.0000226789.51992.3f.
43. Kanekar, A. (2010). Biomarkers predicting progression of human immunodeficiency virus-related disease. J. Clin. Med. Res. *2*, 55–61. https://doi.org/10.4021/jocmr2010.03.255w.
44. Screever, E.M., Yousif, L.I.E., Moslehi, J.J., Salem, J.E., Voors, A.A., Silljé, H.H.W., de Boer, R.A., and Meijers, W.C. (2023). Circulating immune checkpoints predict heart failure outcomes. ESC Heart Fail. *10*, 2330–2337. https://doi.org/10.1002/ehf2.14304.
45. Foks, A.C., and Kuiper, J. (2017). Immune checkpoint proteins: exploring their therapeutic potential to regulate atherosclerosis. Br. J. Pharmacol. *174*, 3940–3955. https://doi.org/10.1111/bph.13802.
46. Kong, Y., Wang, Y., Wu, X., Han, J., Li, G., Hua, M., Han, K., Zhang, H., Li, A., and Zeng, H. (2020). Storm of soluble immune checkpoints associated with disease severity of COVID-19. Signal Transduct. Targeted Ther. *5*, 192. https://doi.org/10.1038/s41392-020-00308-2.
47. Li, W., Syed, F., Yu, R., Yang, J., Xia, Y., Relich, R.F., Russell, P.M., Zhang, S., Khalili, M., Huang, L., et al. (2022). Soluble Immune Checkpoints Are Dysregulated in COVID-19 and Heavy Alcohol Users With HIV Infection. Front. Immunol. *13*, 833310. https://doi.org/10.3389/fimmu.2022.833310.
48. Joseph, J., Premeaux, T.A., Pinto, D.O., Rao, A., Guha, S., Panfil, A.R., Carey, A.J., Ndhlovu, L.C., Bergmann-Leitner, E.S., and Jain, P. (2023). Retroviral b-Zip protein (HBZ) contributes to the release of soluble and exosomal immune checkpoint molecules in

the context of neuroinflammation. J. Extracell. Biol. *2*, e102. https://doi.org/10.1002/jex2.102.

49. Theofilatos, K., Pavlopoulou, N., Papasavvas, C., Likothanassis, S., Dimitrakopoulos, C., Georgopoulos, E., Moschopoulos, C., and Mavroudi, S. (2015). Predicting protein complexes from weighted protein-protein interaction graphs with a novel unsupervised methodology: Evolutionary enhanced Markov clustering. Artif. Intell. Med. *63*, 181–189. https://doi.org/10.1016/j.artmed.2014.12.012.
50. Li, R. (2018). Data Mining and Machine Learning Methods for Dementia Research. Methods Mol. Biol. *1750*, 363–370. https://doi.org/10.1007/978-1-4939-7704-8_25.
51. Rajula, H.S.R., Verlato, G., Manchia, M., Antonucci, N., and Fanos, V. (2020). Comparison of Conventional Statistical Methods with Machine Learning in Medicine: Diagnosis, Drug Development, and Treatment. Medicina *56*, 455. https://doi.org/10.3390/medicina56090455.
52. Zou, Q., Qu, K., Luo, Y., Yin, D., Ju, Y., and Tang, H. (2018). Predicting Diabetes Mellitus With Machine Learning Techniques. Front. Genet. *9*, 515. https://doi.org/10.3389/fgene.2018.00515.
53. Kourou, K., Exarchos, T.P., Exarchos, K.P., Karamouzis, M.V., and Fotiadis, D.I. (2015). Machine learning applications in cancer prognosis and prediction. Comput. Struct. Biotechnol. J. *13*, 8–17. https://doi.org/10.1016/j.csbj.2014.11.005.
54. Kong, J., Ha, D., Lee, J., Kim, I., Park, M., Im, S.H., Shin, K., and Kim, S. (2022). Network-based machine learning approach to predict immunotherapy response in cancer patients. Nat. Commun. *13*, 3703. https://doi.org/10.1038/s41467-022-31535-6.
55. Krittanawong, C., Virk, H.U.H., Bangalore, S., Wang, Z., Johnson, K.W., Pinotti, R., Zhang, H., Kaplin, S., Narasimhan, B., Kitai, T., et al. (2020). Machine learning prediction in cardiovascular diseases: a meta-analysis. Sci. Rep. *10*, 16057. https://doi.org/10.1038/s41598-020-72685-1.
56. Wang, C., Li, Y., Tsuboshita, Y., Sakurai, T., Goto, T., Yamaguchi, H., Yamashita, Y., Sekiguchi, A., and Tachimori, H.; Alzheimer's Disease Neuroimaging Initiative (2022). A high-generalizability machine learning framework for predicting the progression of Alzheimer's disease using limited data. NPJ Digit. Med. *5*, 43. https://doi.org/10.1038/s41746-022-00577-x.
57. Lin, Y., Kim, J., Metter, E.J., Nguyen, H., Truong, T., Lustig, A., Ferrucci, L., and Weng, N.P. (2016). Changes in blood lymphocyte numbers with age in vivo and their association with the levels of cytokines/cytokine receptors. Immun. Ageing *13*, 24. https://doi.org/10.1186/s12979-016-0079-7.
58. Linton, P.J., and Dorshkind, K. (2004). Age-related changes in lymphocyte development and function. Nat. Immunol. *5*, 133–139. https://doi.org/10.1038/ni1033.
59. Franceschi, C., Garagnani, P., Parini, P., Giuliani, C., and Santoro, A. (2018). Inflammaging: a new immune-metabolic viewpoint for age-related diseases. Nat. Rev. Endocrinol. *14*, 576–590. https://doi.org/10.1038/s41574-018-0059-4.
60. Lehallier, B., Gate, D., Schaum, N., Nanasi, T., Lee, S.E., Yousef, H., Moran Losada, P., Berdnik, D., Keller, A., Verghese, J., et al. (2019). Undulating changes in human plasma proteome profiles across the lifespan. Nat. Med. *25*, 1843–1850. https://doi.org/10.1038/s41591-019-0673-2.
61. Raghavan, A., Rimmelin, D.E., Fitch, K.V., and Zanni, M.V. (2017). Sex Differences in Select Non-communicable HIV-Associated Comorbidities: Exploring the Role of Systemic Immune Activation/Inflammation. Curr. HIV AIDS Rep. *14*, 220–228. https://doi.org/10.1007/s11904-017-0366-8.
62. Gandhi, M., Bacchetti, P., Miotti, P., Quinn, T.C., Veronese, F., and Greenblatt, R.M. (2002). Does patient sex affect human immunodeficiency virus levels? Clin. Infect. Dis. *35*, 313–322. https://doi.org/10.1086/341249.
63. Tanaka, T., Basisty, N., Fantoni, G., Candia, J., Moore, A.Z., Biancotto, A., Schilling, B., Bandinelli, S., and Ferrucci, L. (2020). Plasma proteomic biomarker signature of age predicts health and life span. Elife *9*, e61073. https://doi.org/10.7554/eLife.61073.
64. Ribaudo, H.J., Benson, C.A., Zheng, Y., Koletar, S.L., Collier, A.C., Lok, J.J., Smurzynski, M., Bosch, R.J., Bastow, B., and Schouten, J.T.; ACTG A5001/ALLRT Protocol Team (2011). No risk of myocardial infarction associated with initial antiretroviral treatment containing abacavir: short and long-term results from ACTG A5001/ALLRT. Clin. Infect. Dis. *52*, 929–940. https://doi.org/10.1093/cid/ciq244.
65. Krishnan, S., Schouten, J.T., Jacobson, D.L., Benson, C.A., Collier, A.C., Koletar, S.L., Santana, J., Sattler, F.R., and Mitsuyasu, R.; ACTG-ALLRT Protocol Team (2011). Incidence of non-AIDS-defining cancer in antiretroviral treatment-naive subjects after antiretroviral treatment initiation: an ACTG longitudinal linked randomized trials analysis. Oncology *80*, 42–49. https://doi.org/10.1159/000328032.

STAR★METHODS

KEY RESOURCES TABLE

REAGENT or RESOURCE	SOURCE	IDENTIFIER
Critical commercial assays		
Human Immuno-Oncology Checkpoint Protein Panel 1	Millipore Sigma	Cat#HCKP1-11K
Human Immuno-Oncology Checkpoint Protein Panel 2	Millipore Sigma	Cat#HCKP2-11K
suPARnostic ELISA	ViroGates	Cat#E001
LBP Human ELISA	Hycult Biotech	Cat#HK315
Human CD163 Quantikine ELISA	R&D Systems	Cat#DC1630
Human FABP2/I-FABP DuoSet ELISA	R&D Systems	Cat#DY3078
Oxidized LDL ELISA	Mercodia	Cat#10-1143-01
Human Galectin-9 Quantikine ELISA	R&D Systems	Cat#DGAL90
Human IL-6 Quantikine HS ELISA	R&D Systems	Cat#HS600B
Human CD14 Quantikine ELISA	R&D Systems	Cat#DC140
Human CXCL10/IP-10 Quantikine ELISA	R&D Systems	Cat#DIP100
Human TNFRI/TNFRSF1A Quantikine ELISA	R&D Systems	Cat#DRT100
Human TNFRII/TNFRSF1B Quantikine ELISA	R&D Systems	Cat#DRT200
STA-Liatest D-Di Kit	Diagnostica Stago Inc	Cat#NC0233244
Fungitell® Assay	Associates of Cape Cod, Inc.	Cat#FT001
Deposited data		
Python code and statistical approach	Zenodo	https://doi.org/10.5281/zenodo.10635960
ACTG study data	ACTG-158, Data Request	https://member.mis.s-3.net/pss/0
Software and algorithms		
GraphPad Prism v9.5.1	https://www.graphpad.com/features	NA
R environment v4.2.1	https://www.r-project.org/	NA
matrixStats v1.2.0	https://cran.r-project.org/	NA
fda.usc v2.1.0	https://cran.r-project.org/	NA
Python v3.8.8	https://www.python.org/downloads/release/python-3810/	NA

RESOURCE AVAILABILITY

Lead contact

Further information and requests for resources and reagents should be directed to and will be fulfilled by the lead contact, Lishomwa Ndhlovu (lndhlovu@med.cornell.edu).

Materials availability

This study did not generate new unique reagents.

Data and code availability

Individual participant data and a data dictionary defining each field in the set will be made available to investigators on a case-by-case basis via request to Advancing Clinical Therapeutics Globally for HIV/AIDS and Other Infections (ACTG). Completion of an ACTG Data Use Agreement may be required. All original code has been deposited at Zenodo and is publicly available as of the date of publications. DOIs/data applications are listed in the key resources table. Any additional information required to reanalyze the data reported in this paper is available from the lead contact upon request.

EXPERIMENTAL MODEL AND STUDY PARTICIPANT DETAILS

NWCS 411 is a retrospective nested case-control study of PWH that were enrolled in the Advancing Clinical Therapeutics Globally for HIV/AIDS and Other Infections (ACTG) Longitudinal Linked Randomized Trials (ALLRT) cohort from 2001 to 2009. This study examined a multitude of potential predictive biomarkers of inflammation and immune activation and their relationships with NAEs and death.[16] All 401 participants (134 cases, 267 controls), identified from prior ACTG studies, were ART naive when enrolled in an ACTG study, had a plasma HIV RNA level of <400 copies/mL at all subsequent time points (isolated values ≥ copies/mL were allowed if preceding and subsequent values were <400 copies/mL. Participants (or, for minors, their parent or legal guardian) provided written informed consent, and institutional review board approval for ALLRT was obtained by each ACTG site.

Cases were defined as individuals who experienced a myocardial infarction (MI) or a stroke, a non-AIDS-defining malignancy or serious bacterial infection or died from a nonaccidental non-AIDS-related event. The core team previously reviewed and confirmed events.[64,65] Diagnosis of MIs and non–AIDS-defining malignancy outcome (all cancers except Kaposi's sarcoma, B cell non-Hodgkin's lymphoma, primary central nervous system lymphoma and cervical cancer) were collected as part of the parent study and the ALLRT protocols accorded with standard ACTG definitions and reporting criteria. MIs were prospectively reported in each parent study and in ALLRT in the ACTG database and, during parent study follow-up, via the Division of AIDS serious adverse events reporting system. Additionally, standardized reporting criteria that required confirmation via electrocardiogram or elevation in serum myocardial injury enzymes were added to the reporting system. MI diagnoses identified underwent independent review by two study investigators and were classified as definite, possible, or unclassifiable. Investigators were provided with supporting documentation for each MI and details of adverse events occurring within 6 months of the putative MI. A final determination of MIs classified differently by the initial reviewers was made by two additional investigators. Analyses included definite and possible MIs; for subjects with multiple qualifying MIs, only the first event was included. At each clinic visit, site personnel recorded all newly diagnosed malignancies (except squamous cell carcinoma of the skin) on standard ACTG case report forms and were reviewed by two study investigators, which included all supporting data from the case report forms for each malignancy. Additional documentation was requested from the study sites, if required to confirm each diagnosis. Malignancies were classified as prevalent (pre-entry) and incident (post-entry) based on the date of diagnosis.

For each case, up to 3 controls were identified who had an event-free follow-up time equal or greater than the relevant case. Controls were matched on age (within 10 years), sex at time of visit, pre-ART $CD4^+$ T cell count (within 50 cells/mm^3), ART regimen at year 1 (whether it contained a protease inhibitor or abacavir), and parent study.[16]

Stored available plasma specimens obtained from cases and controls at the following 3 time points were evaluated: before ART initiation (hereafter, baseline), 48–64 weeks after initiating ART (hereafter, year 1), and the time point immediately preceding the event for cases and a similar time point for corresponding controls (hereafter, pre-event). The year 1 time point was chosen because by 48 weeks post-ART initiation, all participants were virally suppressed and the slope of decline in activation had stabilized.[42] Plasma samples were available for 156 participants at baseline (64 cases and 92 controls), 263 participants at year 1 (96 cases and 167 controls), and 159 participants at pre-event (58 cases and 101 controls). At each time point, as part of their ACTG study, whole blood was obtained in tubes containing EDTA. Specimens were spun at 400 ×g for 10 min, and plasma was pipetted and spun again at 800 ×g for 10 min. Plasma was aliquoted, frozen, and stored at −70°C until assayed.

METHOD DETAILS

Biomarker quantification

We measured a panel of immunoregulatory proteins in available plasma samples using a custom bead-based multiplex immunoassay according to manufacturer's instructions (Millipore Sigma, HCKP2-11K). Soluble markers measured include the following: 4-1BB (CD137), 4-1BBL (TNFSF9), APRIL (TNFSF13a), Arginase-1, BAFF (B cell activating factor; BLyS; TNFSF13b), CD276 (B7-H3), CD30 (TNFRSF8), CD40L (CD154), CD73 (5′-NT), DNAM-1 (DNAX accessory molecule; CD226), Galectin-1, Galectin-3, ICOSL (inducible T cell co-stimulator ligand; B7-H2), IDO1 (Indoleamine-2,3-deoxygenase 1), OX40 (CD134), PVR (poliovirus receptor; CD155), Siglec-7 (sialic acid-binding Ig like lectin-7; CD328), Siglec-9 (CD329), VISTA (V-type immunoglobulin domain-containing suppressor of T cell activation; B7-H5), and VTCN1 (V-set domain-containing T cell activation inhibitor 1; B7-H4). Data was acquired on a Luminex 200 analyzer and analyzed using MILLIPLEX Analyst software (Millipore). All samples were analyzed in duplicate. Immunoregulatory protein results below the limit of quantification were set to an analytic lower limit. Analytic lower limits were taken as half of the largest lower limit for the specific protein. Any result that was below the identified largest lower limit was also set to the analytic lower limit.

All additional biomarker data were obtained from prior ACTG projects (ALLRT A5001, NWCS 329 and NWCS 387).[16–18] Soluble plasma markers previously analyzed include the following: IL-6 (Interleukin-6), TNFRI (Tumor necrosis factor receptor I), TNFR-II, TLR2 (Toll-like receptor 2), Galectin-9, CD163, CD14, suPAR (Soluble urokinase plasminogen activator receptor), IP-10 (Interferon gamma inducible protein 10), CD40, GITR (Glucocorticoid-induced tumor necrosis factor receptor-related protein), GITRL (GITR ligand), CD80, CD86, CD27, ICOS, CD28, HVEM (Herpesvirus entry mediator), BTLA (B and T lymphocyte attenuator), TIM-3 (T cell immunoglobulin mucin 3), LAG-3 (Lymphocyte-activation gene 3), PD-1 (Programmed death-1), PD-L1 (Programmed death ligand-1), CTLA-4 (Cytotoxic T-lymphocyte associated protein 4; CD152), I-FABP (Intestinal fatty-acid binding protein), BDG (β-D-glucan), LBP (Lipopolysaccharide-binding protein), D-dimer, and oxLDL (Oxidized low-density lipoprotein).

QUANTIFICATION AND STATISTICAL ANALYSIS

Statistical analyses of cohort and biomarker data were performed in Graphpad Prism v9.5.1 or R software v4.2.1. Demographic and clinical characteristics are presented using the median (Q1, Q3) for continuous variables and frequency for categorical variables. To preserve the case-control nature of this dataset for a machine learning platform, conditional transformations for clinical and immunological biomarkers was applied following recommendations by the TEDDY Study Group.[38] Briefly, data was centered within case-control pairings by their means. Differences in data comparing baseline to year 1 were summarized with unpaired non-parametric Hodges-Lehmann estimates and 95% confidence intervals (CIs). Volcano plots were constructed by plotting the negative logarithm of calculated unpaired non-parametric Mann-Whitney test *p*-values and fold difference between cases and controls. Benjamini-Hochberg false discovery rate (FDR) procedure was applied to control for false discoveries in multiple testing.

The relationship between each biomarker and age was assessed using linear regression modeling, adjusted for absolute CD4 T cell count (Biomarker $\sim$ Age+CD4). Adjustment for sex was also considered but was not pursued due to the large proportion of men in the dataset. Separate models were generated for cases and controls using year 1 values. Fitted Gaussian models simulated and tuned 1500 Age/CD4 datapoints to generate predicted biomarker concentrations. Simulated biomarkers were adjusted by mean biomarker concentration within 10 years of age to produce percent change per 10 years age (PC/10). PC/10 was used to create scatterplots with 4-knotted splines and calculate age trajectory fold differences among cases and controls. Inflection points in biomarker age trajectory were calculated using the "matrixStats" and "fda.usc" R packages. Respective min or max age was used when inflection point(s) were not detected.

Machine learning analyses was carried out in Python environment v3.8.8. *Z* score standardization was applied to the dataset prior to employing machine learning algorithms. The standardized dataset comprised of clinical and biological parameters were split into a training and test sets, with one-third of the dataset being reserved for test. To discriminate the case-control status of PWH at each of the pre-ART, 1-year post-ART initiation, and closest pre-event timepoints, we implemented three supervised machine learning models: Support Vector Machine Classifier (SVM), K-Nearest Neighbors (KNN), and extreme gradient boosting (XGBoost). One of highly correlated feature pairs (correlation coefficient $\geq$0.65) were removed. To improve efficiency and accuracy of our models, feature selection was employed to reduce model complexity by selecting optimized features (i.e., biomarkers, demographics, clinical measures) which carry significant and non-redundant predictive power to correctly classify participants. For SVM, Recursive Feature Elimination (RFE) with stratified 2-fold cross validation (CV) was employed. SelectKBest was used for feature selection for KNN. SelectKBest works by retraining the model on K features with the highest values returned by a score function (ANOVA F-value between labels by default). Feature selection and hyperparameter tuning of the XGBoost model (utilizing gbtree booster) was performed using the RFE algorithm and feature importance values in shap-hypetune (version 0.2.4, 'BoostRFE' function). Class imbalance was adjusted for by applying the ratio of the dominant class/minority class to scale_pos_weight within the XGClassifier function of XGBoost. All models were saved using Pickle package. Finally, we plotted the receiver operating characteristic (ROC) and calculated the area under the curve (AUC) to assess a model's capability to distinguish classes. 95% confidence intervals were generated for test dataset following the normal approximation interval of a single training-test split (arxiv.org/abs/1811.12808, "Model Evaluation, Model Selection, and Algorithm Selection in Machine Learning", *Confidence Intervals* via *Normal Approximation*, Sebastian Raschka). All AUC-ROCs are reported along with 95% confidence intervals.